

Brushless Doubly-fed Asynchronous Generator Model for Variable Speed Wind Generation Systems.

F. Blázquez¹, C. Veganzones¹, D. Ramírez¹

¹ Department of Electrical Engineering
E.T.S.I.I. Polytechnic University of Madrid
C/ José Gutiérrez Abascal, 2, 28006 Madrid (Spain)
Phone number:+0034 91 3363178, Fax number:+0034 91 3363008,
e-mail: fblazquez@inel.etsii.upm.es, cveganzones@inel.etsii.upm.es

Abstract. Because of the raising percentage of the wind energy in the total electrical energy, quality control and regulation of the provided energy will be needed for the electrical grid correct functioning. It is only possible using Variable Speed Wind Generation Systems (VSWGS).

In this paper a new electrical generator, Brushless Doubly-Fed Asynchronous Generator (BDFAG) is proposed as a solution for a variable speed wind generation system. The stator of this machine is composed of two balanced three-phase windings with different pole pair number. The rotor is as robust as a conventional squirrel cage, but it has a special design.

A steady state model of a BDFAG. is analyzed. Using this model the power balance in the stator windings and the rotor cage is evaluated. The evaluation results will be experimentally verified with a prototype of BDFAG.

Keywords

Wind energy, special electrical generators, energy conversion

1. Introduction

A. Variable Speed Wind Generation Systems (VSWGS)

An electrical system of a variable speed wind generator is composed of an electrical rotating machine connected to the grid through a power electronic converter. Different technologies for the electrical generator can be used: a synchronous generator as well as a doubly fed asynchronous generator.

The first option (Fig. 1) requires an electronic converter dealing with the whole generator power. In the range of power of the present wind turbines (1MW), the necessary electronic converter switches, working at very low frequencies (800-1000 Hz), produce harmonic currents in the electrical grid [1].

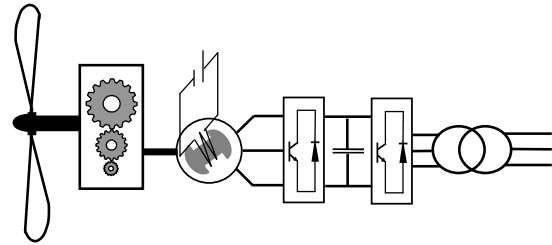


Fig. 1. VSWGS scheme with a conventional synchronous generator

The asynchronous option (Fig.2) requires a fractional power converter in the rotor side (typically 20% of the generator rated power) with a high switching frequency (10-15 kHz), which introduce high quality currents without low harmonic components injected in the electrical grid. This is the main advantage of this system respect the synchronous option.

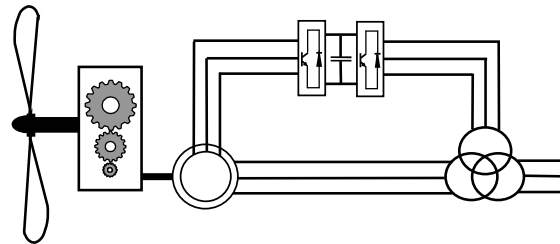


Fig. 2. VSWGS scheme with a conventional doubly fed asynchronous generator

Nevertheless, synchronous machines permit designing with a high number of pole pairs (multipole generators) which means a possible reduction or even the elimination of the gearbox (Fig 3) [2], while this one is always necessary in the doubly fed asynchronous generator.

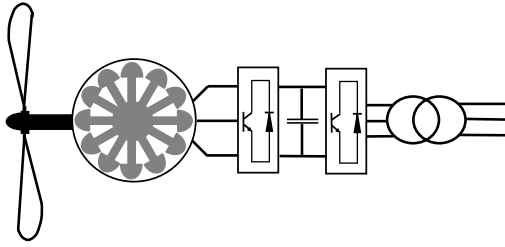


Fig. 3. VSWG scheme with a multipole synchronous generator

B. Brushless Doubly-fed Asynchronous Generator (BDFAG)

The wound rotor asynchronous machine (WRAM) used in VSWG with a conventional doubly fed asynchronous generator has some drawbacks such as:

- 1) *Mechanical problems.* There are some difficulties for the correct mechanical balance of the rotor.
- 2) *Electrical problems,* those appear in the sliding contacts between the rotor rings and the brushes.
- 3) *Maintenance,* which must be more frequent because of the sliding contacts.

In order to avoid these drawbacks a BDFAG instead of WRAM could be used.

The BDFAG has two independent three-phase stator windings: the power winding (p) and the control winding (c). Each one has a different pole pair number, which are p_p and p_c , respectively. The power winding is directly connected to electric grid, so it works with constant frequency ($f_p=50\text{Hz}$), whereas the control winding is fed with a variable frequency (f_c) through a power electronic converter.

With respect to the rotor configuration the conventional squirrel cage design is modified by substituting the original bars for 'nests', which are composed of several concentric loops (Fig. 4):

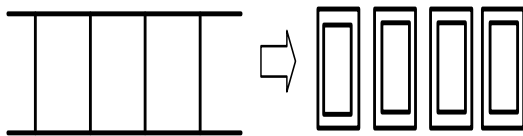


Fig. 4. Rotor configuration example: four nests with two loops by nest.

Its operation is because, for each frequency value of the currents in the control winding, the fields created by both the power and control windings rotate at the same speed with respect to the rotor. Under these conditions, the rotor speed can be expressed [3]:

$$\begin{aligned} \Omega_r &= 2\pi(f_p + f_c)/(p_p + p_c) = \\ &= (\omega_p + \omega_c)/(p_p + p_c) \end{aligned} \quad (1)$$

With this speed, the rotor currents originated from both stator fields have the same frequency. In order to they can be added to each other to compose a single rotor field, the nest number must be [3]:

$$N_b = p_p + p_c \quad (2)$$

This rotor field couples with the two stator windings, thus creating, through the rotor, a 'crossed coupling' between the two stator windings which have different pole number [4].

In this way, the BDFAG is composed of two independent stator windings and a special rotor, which, in spite of not being a conventional squirrel cage, is as robust as this last one. Due to the absence of rotor windings and slip rings, this machine presents the same advantages of the squirrel cage asynchronous generator used in fixed speed generation systems:

- 1) *Easy mechanical balance of the electric generator.*
- 2) *Slight maintenance.*

Moreover, if the stator windings pole number is high, the generation speed values are low (1) and it could carry a possible reduction in the speed relation of the gearbox with the consequent diminution in its weight and size.

Fig. 5 shows the operation scheme of a VSWG with a BDFAG:

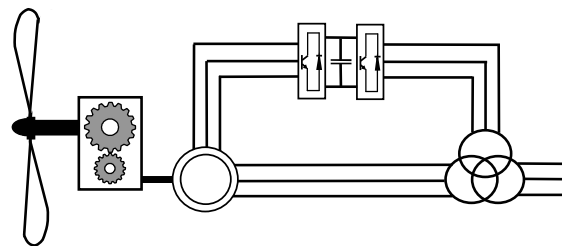


Fig. 5. VSWG scheme with a BDFAG

2. Steady State Model

Next beginning from the steady state basic equations, a complete model is developed in order to establish very clearly the power transfer equations in each winding, in relation to the speed of rotation. These equations will define three performance areas in the BDFAG.

A. Basic Equations of the Model

Reference [3] establishes the space vector equations of BDFAG. Beginning from them and taking into account the different frequencies in each winding, the basic equations of this machine can be expressed:

$$\begin{aligned}\bar{V}_p &= R_p \cdot \bar{I}_p + j \cdot \omega_p \cdot L_p \cdot \bar{I}_p + j \cdot \omega_p \cdot L_{p,r} \cdot \bar{I}_r \\ \bar{V}_c &= R_c \cdot \bar{I}_c + j \cdot \omega_c \cdot L_c \cdot \bar{I}_c + j \cdot \omega_c \cdot L_{c,r} \cdot \bar{I}_r \\ 0 &= R_r \cdot \bar{I}_r + j \cdot X_r \cdot \bar{I}_r + j \cdot \omega_{r,p} \cdot L_{r,p} \cdot \bar{I}_p - j \cdot \omega_{r,c} \cdot L_{r,c} \cdot \bar{I}_c\end{aligned}\quad (3)$$

In these equations $\omega_{r,p}$ and $\omega_{r,c}$ are the angular frequencies of the electromotive forces induced in the rotor winding by the power and control stator fields. These angular frequencies can be expressed in relation to the speed of rotation:

$$\begin{aligned}\omega_{r,p} &= \omega_p - p_p \cdot \Omega_r = \omega_p - p_p \cdot \frac{\omega_p + \omega_c}{p_p + p_c} = \\ &= \frac{\omega_p \cdot p_c - \omega_c \cdot p_p}{p_p + p_c} \\ \omega_{r,c} &= \omega_c - p_c \cdot \Omega_r = \omega_c - p_c \cdot \frac{\omega_p + \omega_c}{p_p + p_c} = \\ &= -\frac{\omega_p \cdot p_c - \omega_c \cdot p_p}{p_p + p_c}\end{aligned}\quad (4)$$

It is define 'rotor current angular frequency' $\omega_r = \omega_{r,p} = -\omega_{r,c}$. Taking into account that $L_{p,r} = L_{r,p}$ and $L_{c,r} = L_{r,c}$, equations (3) can be expressed:

$$\begin{aligned}\bar{V}_p &= R_p \cdot \bar{I}_p + j \cdot \omega_p \cdot L_p \cdot \bar{I}_p + j \cdot \omega_p \cdot L_{p,r} \cdot \bar{I}_r \\ \bar{V}_c &= R_c \cdot \bar{I}_c + j \cdot \omega_c \cdot L_c \cdot \bar{I}_c + j \cdot \omega_c \cdot L_{c,r} \cdot \bar{I}_r \\ 0 &= R_r \cdot \bar{I}_r + j \cdot \omega_r \cdot L_r \cdot \bar{I}_r + j \cdot \omega_r \cdot L_{p,r} \cdot \bar{I}_p + j \cdot \omega_r \cdot L_{c,r} \cdot \bar{I}_c\end{aligned}\quad (5)$$

The interactions between the rotor field and each stator field produce a mechanical torque in the rotor shaft. Each stator field originates a torque component. Each one is proportional to the current absolute value:

$$T_r = p_p \cdot L_{p,r} \cdot \text{Im} \left\{ \bar{I}_p \cdot \bar{I}_r^* \right\} + p_c \cdot L_{c,r} \cdot \text{Im} \left\{ \bar{I}_c \cdot \bar{I}_r^* \right\} \quad (6)$$

B. Power Equations

Beginning from the voltage equation system (5) it can evaluate the distribution of power between the three machine windings (power winding, control winding and rotor winding). These electrical powers can be related with the mechanical power in the shaft whose value is obtained by multiplying the torque (6) and the rotor speed (1). In this process, the core loss power is not considered.

Multiplying by \bar{I}_p^* , \bar{I}_c^* and \bar{I}_r^* the equations (3) and taking the real part of the resultant expressions, it is obtained:

$$\begin{aligned}\text{Re} \left(\bar{V}_p \cdot \bar{I}_p^* \right) &= R_p \cdot I_p^2 + \text{Re} \left(j \cdot \omega_p \cdot L_{p,r} \cdot \bar{I}_r \cdot \bar{I}_p^* \right) \\ \text{Re} \left(\bar{V}_c \cdot \bar{I}_c^* \right) &= R_c \cdot I_c^2 + \text{Re} \left(j \cdot \omega_c \cdot L_{c,r} \cdot \bar{I}_r \cdot \bar{I}_c^* \right) \\ 0 &= R_r \cdot I_r^2 + \text{Re} \left(j \cdot \omega_r \cdot L_{p,r} \cdot \bar{I}_p \cdot \bar{I}_r^* \right) + \text{Re} \left(j \cdot \omega_r \cdot L_{c,r} \cdot \bar{I}_c \cdot \bar{I}_r^* \right)\end{aligned}\quad (7)$$

They are defined the slips respect to the power and control fields, s_p and s_c :

$$s_p = \frac{\omega_p - p_p \cdot \Omega_r}{\omega_p} \quad s_c = \frac{\omega_c - p_c \cdot \Omega_r}{\omega_c} \quad (8)$$

Taking into account (4) and (8), the equation (7c) can be expressed:

$$\begin{aligned}R_r \cdot I_r^2 &= s_p \cdot \text{Re} \left(j \cdot \omega_p \cdot L_{p,r} \cdot \bar{I}_r \cdot \bar{I}_p^* \right) + \\ &+ s_c \cdot \text{Re} \left(j \cdot \omega_c \cdot L_{c,r} \cdot \bar{I}_r \cdot \bar{I}_c^* \right)\end{aligned}\quad (9)$$

Next, the mechanical power is evaluated:

$$P_{mec} = T_r \cdot \Omega_r \quad (10)$$

The rotor speed in relation to the slips s_p and s_c (8), is:

$$\Omega_r = \frac{1-s_p}{p_p} \cdot \omega_p \quad \Omega_r = \frac{1-s_c}{p_c} \cdot \omega_c \quad (11)$$

Multiplying (6) by (11), it is obtained the next expression for the mechanical power:

$$\begin{aligned}P_{mec} &= (1-s_p) \cdot \text{Re} \left(j \cdot \omega_p \cdot L_{p,r} \cdot \bar{I}_r \cdot \bar{I}_p^* \right) + \\ &+ (1-s_c) \cdot \text{Re} \left(j \cdot \omega_c \cdot L_{c,r} \cdot \bar{I}_r \cdot \bar{I}_c^* \right)\end{aligned}\quad (12)$$

In the last expressions, it is designated:

$$\begin{aligned}P_p &= \text{Re}(\bar{V}_p \cdot \bar{I}_p^*) \\ P_c &= \text{Re}(\bar{V}_c \cdot \bar{I}_c^*)\end{aligned}$$

to the power handled in the power and control windings,

$$\begin{aligned}P_{pCu} &= R_p \cdot I_p^2 \\ P_{cCu} &= R_c \cdot I_c^2 \\ P_{rCu} &= R_r \cdot I_r^2\end{aligned}$$

to the loss power produced in the power winding, control winding and rotor winding,

$$P_{p\delta} = \operatorname{Re}(j \cdot \omega_p \cdot L_{p,r} \cdot \bar{I}_r \cdot \bar{I}_p^*)$$

$$P_{c\delta} = \operatorname{Re}(j \cdot \omega_c \cdot L_{c,r} \cdot \bar{I}_r \cdot \bar{I}_c^*)$$

$$\Omega_n = \frac{\omega_p}{p_p + p_c}$$

to the fraction of the stator winding power that crosses to the rotor through the air-gap.

Taking into account all these expressions, the equations (7), (8) and (12) can be written:

$$P_p = P_{pCu} + P_{p\delta}$$

$$P_c = P_{cCu} + P_{c\delta}$$

$$P_{rCu} = s_p \cdot P_{p\delta} + s_c \cdot P_{c\delta} \quad (13)$$

$$P_{mec} = (1 - s_p) \cdot P_{p\delta} + (1 - s_c) \cdot P_{c\delta}$$

This formulation lets a very adequate explanation of the BDFAG performance in different conditions of torque and speed.

C. Performance Areas. Definition

According to (1) the BDFAG speed only depends on the angular frequencies of the currents circulating into the stator windings, and this speed not depends on the shaft torque. Nevertheless, the power distribution and the power flux direction in each machine winding depend on the performance speed (13).

Two characteristic performance speeds are defined for the BDFAG.

- 1) *Upper limit speed* (Ω_L), is the BDFAG performance speed when the angular frequency in the control winding is equal to:

$$\omega_c = \omega_p \cdot \frac{p_c}{p_p} = \omega_L$$

With this angular frequency (ω_L), the BDFAG speed is: (1)

$$\Omega_L = \frac{\omega_p}{p_p}$$

and the slips (8):

$$s_p = s_c = 0$$

- 2) *Natural speed* (Ω_n), is the BDFAG performance speed when the control winding is fed with direct current:

$$\omega_c = 0$$

Under these conditions, the BDFAG speed is equal to: (1)

and the slips (8):

$$s_p = \frac{P_c}{p_p + p_c}, \quad s_c \rightarrow +\infty$$

These two speeds are the borders of three performance areas. At these speeds, the slips respect to the power and control fields, s_p and s_c , change their signs. Because of this reason, the power flux is different in each performance area.

The three defined performance areas are:

- 1) *AREA A*, that includes the speeds higher than Ω_L . These speeds are achieved if the angular frequency in the control winding:

$$\omega_c > \omega_L$$

In this area, the slips (8) are included in the next intervals:

$$0 > s_p > -\infty$$

$$0 < s_c < \frac{p_p}{p_p + p_c} \quad (14)$$

- 2) *AREA B*, that includes the speeds between Ω_n and Ω_L . These speeds are achieved if the angular frequency in the control winding:

$$0 < \omega_c < \omega_L$$

Under this condition, the slips (8) are included in the next intervals:

$$\frac{p_c}{p_p + p_c} > s_p > 0$$

$$-\infty < s_c < 0 \quad (15)$$

- 3) *AREA C*, that includes the speeds lower than Ω_n . In order to achieve these speeds is need to feed the control winding with reverse sequence angular frequencies:

$$\omega_c < 0$$

When $\Omega_r = 0$, the slips are equal to:

$$s_p = s_c = 1$$

Therefore, in this performance area, the slips are included in the intervals:

$$1 > s_p > \frac{P_c}{P_p + P_c} \quad (16)$$

$$1 < s_c < \infty$$

Fig. 6 indicates the speed, angular frequency and slip values in each performance area (A, B and C) that have just been defined:

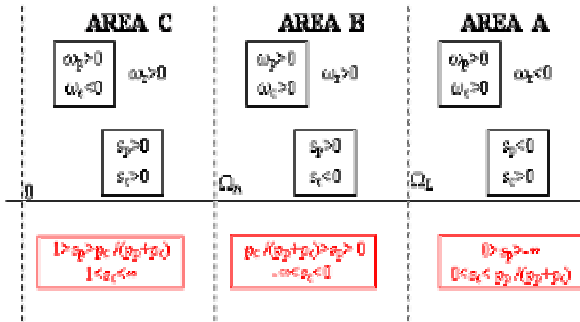


Fig. 6. Performance Areas

D. Performance Areas. Power Transference

Now it is going to analyse the power transference between the BDFAG windings in relation to the slips s_p and s_c . In order to make the analysis the power equations (13) are applied.

1) AREA A. According to (14) in this area

$$s_p < 0 \quad , \quad 1 - s_p > 0 \quad (>1)$$

$$s_c > 0 \quad , \quad 1 - s_c > 0 \quad (<1)$$

With these slip values if the loss term (P_{rCu}) is underestimated, the equation (13c) determinates that $P_{p\delta}$ and $P_{c\delta}$ have the same sign. In the generator performance $P_{mec} < 0$ and $P_{p\delta}, P_{c\delta} < 0$, then:

$$\rightarrow s_p \cdot P_{p\delta} > 0, \quad (1 - s_p) \cdot P_{p\delta} < 0, \quad P_p < 0$$

$$\rightarrow s_c \cdot P_{c\delta} < 0, \quad (1 - s_c) \cdot P_{c\delta} < 0, \quad P_c < 0$$

Fig. 7 shows the power transference direction in this area:

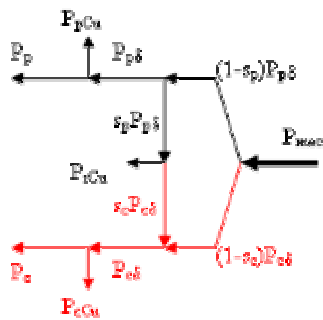


Fig. 7. Power Transference in Area A

2) AREA B. According to (15) in this area

$$s_p > 0 \quad , \quad 1 - s_p > 0 \quad (<1)$$

$$s_c < 0 \quad , \quad 1 - s_c > 0 \quad (>1)$$

With these slip values if the loss term (P_{rCu}) is underestimated, the equation (13c) determinates that $P_{p\delta}$ and $P_{c\delta}$ have the same sign in this area, too. In the generator performance $P_{mec} < 0$ and $P_{p\delta}, P_{c\delta} < 0$, then:

$$\rightarrow s_p \cdot P_{p\delta} < 0, \quad (1 - s_p) \cdot P_{p\delta} < 0, \quad P_p < 0$$

$$\rightarrow s_c \cdot P_{c\delta} > 0, \quad (1 - s_c) \cdot P_{c\delta} < 0, \quad P_c < 0$$

Fig. 8 shows the power transference direction in this area:

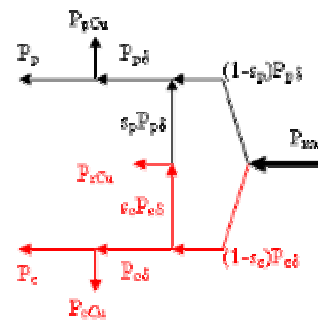


Fig. 8. Power Transference in Area B.

3) AREA C. According to (16) in this area:

$$s_p > 0 \quad , \quad 1 - s_p > 0 \quad (<1)$$

$$s_c > 0 \quad , \quad 1 - s_c < 0$$

With the same reasoning that it has been used in the previous areas, it is inferred that $P_{p\delta}$ and $P_{c\delta}$ have different signs. In the generator performance $P_{mec} < 0$, with $P_{p\delta} < 0$ and $P_{c\delta} > 0$:

$$\rightarrow s_p \cdot P_{p\delta} < 0, \quad (1 - s_p) \cdot P_{p\delta} < 0, \quad P_p < 0$$

$$\rightarrow s_c \cdot P_{c\delta} > 0, \quad (1 - s_c) \cdot P_{c\delta} < 0, \quad P_c > 0$$

Fig. 9 shows the power transference direction in this area:

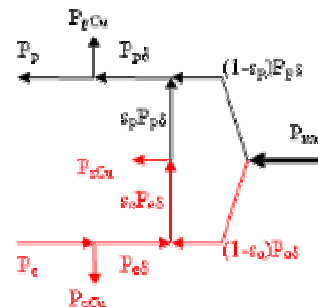


Fig. 9. Power Transference in Area C

So then, the generator's behaviour is different over and below of the natural speed Ω_n . If $\Omega_r > \Omega_n$, for both areas A and B the converter fixes a direct sequence system ($\omega_c > 0$) in the control winding. In these conditions, the BDFAG generates electrical power through both stator windings. However, the inner power flux is different in areas A and B.

If $\Omega_r < \Omega_n$ (area C) the converter fixes a reverse sequence system ($\omega_c < 0$). Now, the BDFAG generates electrical power through the power winding but the control winding consumes electrical power.

3. Experimental Results

A. Prototype description

Based upon the structure of a conventional machine, which has 36-slots stator sheets and 28-slots rotor sheets, a prototype with the following characteristics has been built:

- Power stator winding with 5 pole pairs
- Control stator winding with 2 pole pairs
- Rotor winding with $5+2=7$ nests

The choice of the pole pairs number in the power and control windings - $p_p=5$ and $p_c=2$ - is the result of a theoretical study presented in [5].

- 1) *Stator windings.* A double layer configuration has been chosen, for power and control stator windings. Each winding is distributed through all the stator slots, occupying them partially. Fig. 10 shows a photograph of the prototype's stator, as well as a detailed diagram of the windings disposition in the slots.

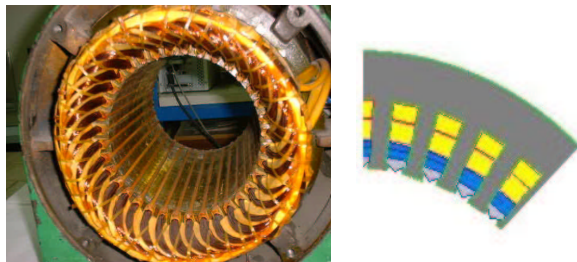


Fig. 10. Prototype's stator

- 2) *Rotor electrical circuit.* Each of the 7 nests is formed by two concentric loops made up of copper strap mechanized with the same shape as the slot. The loops are electrically isolated from the rotor core with several insulating paper layers. Fig. 11 shows a photograph and a diagram of the electric circuit in the prototype's rotor.

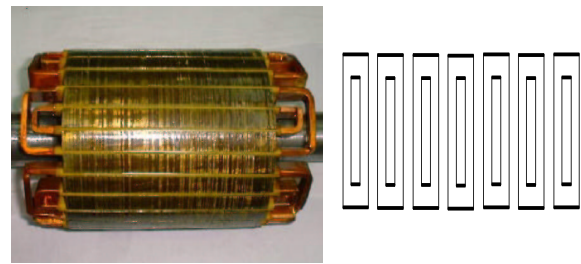


Fig. 11. Prototype's rotor

B. Test workbench

In order to carry out the tests, they are needed three power sources. Two of them are electrical power sources to feed the control winding and the power winding. The other one is a 'mechanical source' that it is joined to the rotor shaft.

- 1) *Source of the power winding.* It is used a three-phase autotransformer in order to obtain a variable voltage level at $f_p=50\text{Hz}$.
- 2) *Source of the control winding.* The harmonic distortion that an electronic converter introduces it could have influence in the test measurements.

In order to avoid this influence it has developed a sinusoidal three-phase source that it has a variable voltage level and variable frequency. A synchronous generator constitutes this source. The generator is droved by a direct current motor.

- 3) *Mechanical Drive.* A direct current machine has been chosen in order to get a perfect adjustment of the mechanical torque. An electronic converter, that it fixes the electromagnetic torque, feeds the direct current machine.

Fig. 12 shows the assembly used in the tests.



Fig. 12. Tests workbench

C. Test results

The goal of the tests is to prove two essential characteristics in the generator's performance:

- The speed does not depend on the generator's load.
- The power flux is according to the theory.

Satisfactory results have been obtained in the three performance areas (A, B and C). Now the results in area C are shown. This area is the most interesting in VSWG because of the low performance speeds.

1) Frequency in the control winding $f_c = -15 \text{ Hz}$

With this feeding frequency, the theoretical speed according to (1) is:

$$n_r = 300 \text{ r/min}$$

Feeding the power winding at $U_p=250\text{V}$ and the control winding at $U_c=219\text{V}$, the BDFAG has been subjected to several loads. TABLE I shows the obtained results:

TABLE I. – $f_c = -15\text{Hz}$ Tests Results

CONTROL WINDING		POWER WINDING		SPEED (r/min)
Q _c (VAR)	P _c (W)	P _p (W)	Q _p (VAR)	
150,92	62	-36,06	408,76	300
165,96	74,6	-70,7	460,52	301
181,23	88,8	-101,9	512,92	300
188,31	99,6	-118,7	553,71	300
191,22	111,8	-133,4	594,34	301
202,88	126,8	-142,9	649,36	300
208,01	140,6	-148,3	707,76	300

2) Frequency in the control winding $f_c = -10 \text{ Hz}$

With this feeding frequency, the theoretical speed according to (1) is:

$$n_r = 342,86 \text{ r/min}$$

Feeding the power winding at $U_p=250\text{V}$ and the control winding at $U_c=167\text{V}$, the BDFAG has been subjected to several loads. TABLE II shows the obtained results:

TABLE II. – $f_c = -10\text{Hz}$ Tests Results

CONTROL WINDING		POWER WINDING		SPEED (R/MIN)
Q _c (VAR)	P _c (W)	P _p (W)	Q _p (VAR)	
179,15	75,1	-96,04	413	342
170,97	75,8	-109,3	441,14	342
173,43	80,5	-123	459	342
167,4	83,8	-133,3	486,58	343
160,8	85,6	-141,7	530,94	343
160,95	89,7	-151,4	558,28	342
161,93	96,2	-158,4	601,42	343
166,16	103,8	-167,5	636,09	342
169,8	111,1	-160,2	698,63	342

D. Analysis

The first important result in the TABLES I and II is that the speed values are according to (1) and they are not depends on the generator's load. The differences between the measured speeds (TABLES I, II. Column 5) and the theoretical speeds are lower than 0.34 per cent. This error value is perfectly imputable to the system of measurement.

For the measure of the power in both windings, it has used a wattmeter with motor reference connection. In this way, if the value of the measurement is positive it indicates that the winding consumes electrical power. If the value is negative, it indicates that the winding gives up electrical power.

So then, the power flux direction is according to the theory that it has been developed in point 2. When the BDFAG works in area C, it gives up electrical power through the power winding and it consumes electrical power through the control winding (Fig. 9).

4. Conclusions

In this paper the steady state equations of a BDFAG has been presented. Beginning from them, it has defined three different performance areas and it has studied the power transference between all windings.

Because of the low speed, one of the performance areas (area C) could be very adequate to use the BDFAG in VSWG.

Several tests with a BDFAG prototype has been carried out in order to contrast the proposed theory. These tests have proved that the performance in area C is possible.

Nevertheless in order to obtain decisive results, it would be needed a model that it takes into account the loss power in the magnetic core.

Symbols

- p_p, p_c pole pair numbers of the power and control windings
- f_p, f_c frequencies of the power and control windings
- Ω_r rotor speed
- N_b number of nests
- V_p, V_c voltages of the power and control windings
- I_p, I_c currents of the power and control windings
- I_r rotor current
- R_p, R_c resistance of the power and control windings
- R_r rotor resistance
- L_p, L_c self-inductance of the power and control windings
- X_r rotor reactance
- L_{pr}, L_{cr} mutual inductance
- ω_p, ω_c angular frequencies of the power and control windings
- T_r electromagnetic torque

References

- [1] M. Lafoz, JI Iglesias, C. Veganzones. Procc. Conference EPE-2000. Dublin (S) August 2000
- [2] C. Veganzones; F. Blázquez A. Alonso et als. "Comparative Study of several Alternatives of Multipole Generator for MW Direct Driven Wind Turbines" Procd. of 2000-European Union Wind Energy Congress (EUWEC-2000) Kassel (Germany) Sep 2000
- [3] Willianson S., Ferreira A.C., Wallace A.K., "Generalised theory of brushless double fed machine. Part 1 Analysis", IEE Proc Electric. Power Appl. Vol 144, n2, pg 111-122, Mach 1997.
- [4] Wiedenbrüg, Boger, Wallace. "Electromagnetic Mechanism of Synchronous Operation of the Brushless Doubly-Fed Machine" Industry Applications Conference, 1995 IEEE
- [5] F. Blázquez; C. Veganzones; D. Ramírez; J. R. Arribas; M.Lafóz; "Brushless Doubly-fed Asynchronous Generator for Variable Speed Wind Generation Systems" International Conference on Electrical Machines. ICEM'02. Brujas, Ag. 2002.